Journal of Microscopy, Vol. 230, Pt 1 2008, pp. 48–60
Received 9 July 2007; accepted 9 October 2007

Spatial control of pa-GFP photoactivation in living cells

I. TESTA*‡, D. PARAZZOLI†, S. BAROZZI†, M. GARRÈ‡, M. FARETTA† & A. DIASPRO*‡§¶
**Department of Physics, University of Genoa, I-16146 Genoa, Italy*
†European Institute of Oncology, Department of Experimental Oncology, 20141 Milan, Italy
‡LAMBS-MicroScoBio Research Center, University of Genoa, 16146 Genoa, Italy
§IFOM, Istituto FIRC di Oncologia Molecolare, 20139 Milan, Italy
¶IBF-CNR, National Research Council, I-16149 Genoa, Italy

Key words. Confocal microscopy, GFP, pa-GFP, TIRF, two-photon excitation microscopy, 3D fluorescence microscopy.

Summary

Photoactivatable green fluorescent protein (paGFP) exhibits peculiar photo-physical properties making it an invaluable tool for protein/cell tracking in living cells/organisms. paGFP is normally excited in the violet range (405 nm), with an emission peak centred at 520 nm. Absorption cross-section at 488 nm is low in the not-activated form. However, when irradiated with high-energy fluxes at 405 nm, the protein shows a dramatic change in its absorption spectra becoming efficiently excitable at 488 nm. Confocal microscopes allow to control activation in the focal plane. Unfortunately, irradiation extends to the entire illumination volume, making impracticable to limit the process in the 3D (three-dimensional) space. In order to confine the process, we used two advanced intrinsically 3D confined optical methods, namely: total internal reflection fluorescence (TIRF) and two-photon excitation fluorescence (2PE) microscopy. TIRF allows for spatially selected excitation of fluorescent molecules within a thin region at interfaces, i.e. cellular membranes. Optimization of the TIRF optical set-up allowed us to demonstrate photoactivation of paGFP fused to different membrane localizing proteins. Exploitation of the penetration depth showed that activation is efficiently 3D confined even if limited at the interface. 2PE microscopy overcomes both the extended excitation volume of the confocal case and the TIRF constraint of operating at interfaces, providing optical confinement at any focal plane in the specimen within subfemtoliter volumes. The presented results emphasize how photoactivation by non-linear excitation can provide a tool to increase contrast in widefield and confocal cellular imaging.

Correspondence to: Alberto Diaspro. Tel: +390103536426; e-mail: diaspro@fisica.unige.it

Introduction

Fluorescence microscopy, including the advent of green fluorescent protein (GFP) and of two-photon excitation (2PE) microscopy, has acquired enormous success in biology and medicine applications moving towards the nanoscale level (Yuste, 2005; Willig *et al.*, 2006). Within this scenario, fluorescence recovery after photobleaching (FRAP)-based assays are nowadays routinely used to study molecular motion of proteins in living cells (Lippincott-Schwartz *et al.*, 2003). Next to photobleaching, photoactivation has been successfully employed to track particles highlighting structures over a dark background (Lippincott-Schwartz *et al.*, 2003; Patterson & Lippincott-Schwartz, 2004). New fluorescent proteins derived from targeted point mutation in the Aequorea Victoria Green Fluorescent Protein DNA sequence, such as the paGFP (Patterson & Lippincott-Schwartz, 2002), or synthesized from other organisms, as in the case of Kaede (Mutoh *et al.*, 2006; Sato *et al.*, 2006) and PSCFP (Chudakov *et al.*, 2004), have contributed to the set-up of protocols based on controlled photoactivation of selected regions of interest within the specimens being studied. Unfortunately, molecular diffusion inside cells can compromise the result of the marking procedure. Self-organized structures are originated by the maintenance of a local density gradient based on chemical interaction affinity with a frequent exchange of molecules with external compartments (Misteli, 2001). In these conditions, permanent labelling by photoactivation is not achievable, because photolabelled molecules will be periodically replaced due to the above-mentioned flux. Even in this case, photoactivation protocols can be successfully employed to study the diffusion rate by switching on selected areas and studying the increase in fluorescence in and out of the activated compartment (Beaudouin *et al.*, 2006; Thoumine *et al.*, 2006).

The usually employed experimental set-ups comprise widefield microscopes eventually equipped with external laser sources, and confocal microscopes (Conchello & Lichtman, 2005). Such optical set-ups demonstrate the limitation of a loss of 3D confinement, i.e. along the optical axis. Even if confocal microscopy is able to produce optical slices to perform an intracellular tomography, optical sectioning is achieved by filtering out emitted light coming from planes lying above and below the plane of focus. Excitation light focused on the sample spans over a thickness essentially determined by the objective illuminating cone, delivering a relevant amount of energy out of the plane of interest and consequently causing uncontrolled photobleaching or photoactivation over a height of several micrometres, even if the planar confinement can be reduced to a single diffraction limited spot of 180–200 nanometres.

Optical techniques based on limiting the illuminated volume to increase spatial resolution can consequently be very effective in controlling fluorescence photoactivation or photoconversion. Total internal reflection fluorescence (TIRF) microscopy exploits the variation of refractive index at the interface between two media, resulting in an evanescent electromagnetic field, to prime fluorescence excitation of molecules located within few hundreds nanometres from the glass cover slip (Axelrod, 2003). Here, light intensity decreases exponentially moving away from the surface allowing for a physical confinement of the excitation dependently on the employed wavelength and incident angle at the interface. In the case of a cell deposited on a glass slide, the achievable signal-to-noise ratio grants efficient visualization of its basal membrane down to a single molecule sensitivity (Sako *et al.*, 2003). The most relevant limitation of TIRF microscopy is given by its inherent inability to operate apart from the basal membrane, i.e. to penetrate into the cell as in optical sectioning-based techniques. Non-linear excitation techniques, such as 2PE laser scanning microscopy, allow to overcome this restriction providing a real 3D reconstruction ability based on a true spatial confinement within the whole volume occupied by the specimen (Diaspro *et al.*, 2005). Two-photon absorption is, according to the rules of quantum mechanics, a low probability event requiring an incredibly high amount of photons. Consequently, only those fluorescent molecules positioned in the optical focal plane of the microscope objective will be excited by the simultaneous absorption of two low-energy photons. Rapid decay of excitation efficiency away from the objective focus provides an intrinsic spatial confinement ability that can be put into practice both for fluorescence stimulation and photoactivation.

In the present paper, we describe photoactivation protocols based on TIRF and 2PE microscopy demonstrating how spatial control of the photon distribution can be employed to efficiently confine fluorescence activation in three dimensions. Optical thickness of the activated volume can be limited to subresolution distances when evanescent fields are employed as well as two-photon interactions can be used to confine the photoactivation process in different cellular compartments. The main advantage arising from the utilization of two-photon photoactivation, despite its lower spatial resolution, lies in the chance of priming the process in a selective way within the whole 3D space occupied by the sample. 3D confined photoactivation can consequently provide novel insights in the study of molecular dynamics in living cells, thus allowing for the development of *ad hoc* protocols for accurate structure photoprinting and molecular motion characterization.

Materials and methods

Cell culture, transfection and DNA probes

Human U2OS and HeLa cells were grown on glass cover slips under standard cell culture conditions at 37°C, 5% CO_2 in a DMEM medium supplemented with 10% North American foetal bovine serum (Gibco Europe, Paisley, U.K.). The paGFP N1 encoding DNA was a generous gift from Dr. George Patterson. Transient transfection was performed using a FuGene (Boehringer-Ingelheim Italia S.p.A., Milan, Italy) reagent according to manufacturer instructions.

EGFR-paGFP (paGFP at the C terminus of the receptor) plasmid has been obtained by replacing the eGFP moiety in a pcDNA3 EGFR-GFP encoding DNA. The paGFP coding fragment has been obtained by PCR amplification from the paGFP N1 plasmid and inserted into the EGFR encoding vector.

SHCp52-paGFP has been obtained by cloning the SHCp52 fragment into the paGFP N1 encoding DNA. The same approach has been followed for H2B-paGFP cloning.

Cells were harvested and observed or fixed after 48 h. For TIRF microscopy, cover slips were put onto a specific holder and immersed in PBS to maintain the correct refractive index necessary for evanescent field creation. Living cells measurements were performed in cell culture medium at room temperature (about 26°C).

TIRF microscopy

TIRF imaging of cells was performed by an Olympus TIRF workstation based on CellR̂ Imaging System (Olympus Europe, Munich, Germany). A 405-nm laser diode, 488-nm Ar laser and 568-nm Kr laser were coupled into an inverted epifluorescence Olympus IX81 motorized microscope, and focused at an off-axis position of the objective back focal plane; cells plated on glass cover slips were viewed through a high-aperture 60× objective lens (UIS2 60× TIRFM PlanApo N, NA 1.45, Olympus, Tokyo, Japan) with an additional 1.6× magnification lens. For paGFP imaging, a 505-nm dichroic mirror together with a 515–550 nm emission filter was employed. Images (12-bit depth) were acquired using an Orca-ER cooled CCD digital camera (Hamamatsu Italy, Milan, Italy).

The coupling of the violet excitation (405 nm) source has been optimized to get the maximal laser power in the focal plane

of the objective for photoactivation studies. Consequently, a direct coupling through air into the TIRF condenser for the 405-nm laser line has been adopted avoiding the use of optical fibres and the associated loss in energy transmission. Optics has also been selected in order to maximize violet energy output. Two different objectives have been evaluated to select the transmission rate, namely: a standard 60× 1.45 NA Olympus TIRF objective and a 60× 1.45 NA UIS2 TIRF objective with enhanced transmission in the violet range. The first one allows to deliver about 2 mW out of the 25 mW available by the diode, whereas the second one grants an increased transmission of 2.7 mW, as measured with a power metre positioned in front of the objective lens. Increased scattering has been detected through an evaluation of the image haze under these observation conditions.

The multiple TIRF-condensers set-up allows to simultaneously select the optimal incident angle for activation (405 nm) and excitation (488 nm) of paGFP signal independently from the excitation wavelength and to rapidly switch between photoactivation and imaging under TIRF conditions. Set-up of the total internal reflection conditions has been evaluated both by qualitative examination of the acquired images by maximization of contrast and minimization of out of focus light thanks to the focusing on the basal layer plane. Parallel recording of the reflected light intensity has been performed to confirm reaching of the critical angle. Critical angle illumination for the violet laser line has been further checked by comparison with the 488-nm illumination TIRF image for the equivalence of the acquired data. Illumination angle was further increased to grant minimal penetration depth and reduced light scattering. Activation under non-total internal reflection conditions was tested showing increasing of out-of-focus light due to activated fluorescence in the inner cell compartment. ImageJ image-analysis software (W. Rasband, National Institute of Health, Bethesda, MD) was used for data analysis.

Confocal laser scanning microscopy

Photoactivation measurements were performed on a Leica TCS SP2 confocal microscope equipped with a 63×/1.40 (OIL CS HC×PL APO) objective lens (Leica), employing the 405-nm line of a 20-mW laser diode. Imaging of paGFP pre- and post-activation was obtained by the 488-nm laser line of a 20-mW Argon laser. The spectral window used to collect fluorescence spanned from 500 to 600 nm. For measurement of TIRF activation depth, fixed cells were first activated on the TIRF microscope and then retrieved on the confocal microscope. Cells were plated on grided cover slips (175-μm grid size, Eppendorf, Germany), fixed and activated in selected grid regions on the TIRF microscope and then moved to the confocal microscope. Once identified the activation area, single cells were located by eye inspection. Comparison of CCD data from TIRF and confocal sections of the basal membrane (with identical spatial sampling) has been performed to obtain a rough-image realignment.

Two-photon excitation microscopy

A Chameleon-XR (Coherent, Santa Clara, CA) Ti:Sapphire laser source was directly coupled into the scanning head of a Leica TCS SP2 AOBS confocal microscope using an infrared port. Pulse width lies within the range of 140 fs full width at half maximum at a repetition frequency of 90 MHz at the laser output window. Measurements were carried out using an average power of $\langle P\rangle_{min} = 2.5$ mW up to $\langle P\rangle_{max} = 12.5$ mW at the focal plane for two-photon-induced photoactivation. Imaging of the activated proteins was obtained using the 488-nm line of a 20-mW Argon ion laser. Images were collected using a 100 × oil N.A. = 1.4 objective HCX PL APO (Leica Microsystems S.p.A., Milan, Italy). The two-photon activation process on living cells was first primed by focusing a pulsed infrared laser beam on a region of the sample with $\lambda = 750$ nm. Subsequently, the de-zoomed area was excited with $\lambda = 488$ nm and $\langle P\rangle = 0{,}04$ mW (before the objective) to track the activated proteins. The spectral window used for collecting fluorescence was 500–600 nm.

Results

Photoactivation by focused Gaussian laser beam cannot be confined along the optical axis

Acousto-Optical Tunable Filters and/or dynamic field of view adjustment by scanning mirrors reorientation allow for efficient point-by-point modulation of laser power providing a precise confinement of activation along the xy coordinates of the objective focal plane. To check for the real spatial extension of the activated region, HeLa cancer cells were transfected to express H2B-paGFP fusion protein. Due to the low-diffusion constant *(17)* of the protein, diffusion effects were negligible on the time scale of the experiment and the activation profile along the three dimensions can be clearly estimated. Four circular regions of interest (1 μm diameter) were sequentially activated at maximum 405 nm laser output with a pixel dwell time of 2.5 μsec (Fig. 1). The photoactivation process is clearly evidenced by a comparison of the irradiated area upon illumination at low 405 nm power for imaging (AOTF value: 10%) and at 488 nm: the molecules in the targeted ROIs lose the ability to absorb photons in the violet range in comparison to their original state (Fig. 1 panel A 405 nm pre- and post-activation) while increasing enormously their cross-section towards 488 nm light as demonstrated by the high contrast produced upon activation (Fig. 1 panel A 488 nm post-activation: Green Area in comparison to the rest of the nuclear region). Panel B and C evidenced the

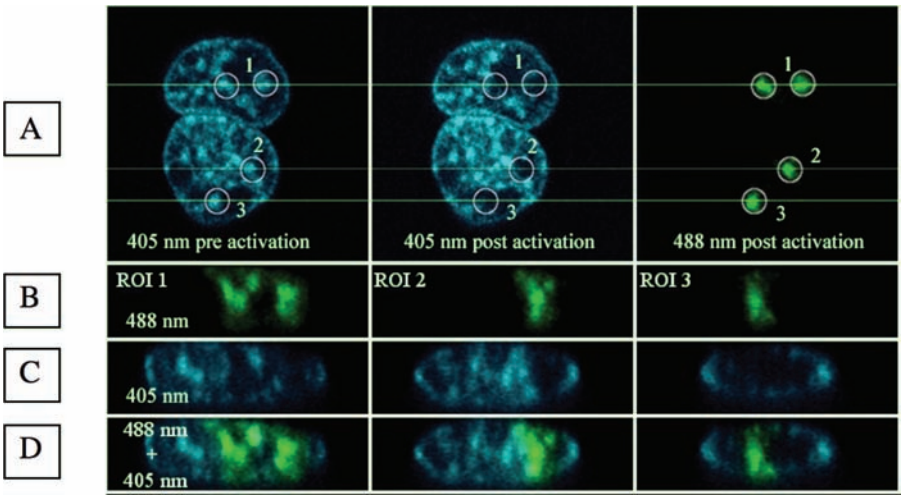

Fig. 1. Spatial extension of photoactivated volumes by Gaussian laser beam. HeLa cells expressing H2B-paGFP fusion protein were photoactivated in conventional confocal microscopy. Panel A. Low-energy 405-nm irradiation was employed to visualize histone distribution (405-nm pre-activation) and targeting specific region of interest (white circles: 1, 2, 3). Full energy illumination with violet radiation induced photoconversion increasing the 488 nm (488-nm post-activation) and reducing the 405-nm (405-nm post-activation) absorbance peak in the specific region of interest. Panel B. XZ plane sectioning at 488 nm across the lines depicted in panel A through the activated ROIs. Each column reports the result for the three different ROIs. The spatial extension of the photoactivation process along the optical axis is clearly evidenced demonstrating that the thickness of the photoconverted area essentially covers the entire nucleus depth. Panel C. The same as in panel B but visualized at low 405-nm power to demonstrate the spectral photoconversion. The activated volumes now appear dark due to the reduced absorbance peak in the violet range. Panel D. Colour merge of the XZ views in panel B and C. The superposition of colour-evidenced area where the delivered energy was not sufficient to activate all the irradiated molecules. A mixed population of paGFP proteins absorbing light both at 405 and 488 nm was consequently present.

axial extension of the activated regions (ROI1: first column; ROI 2: second column; ROI 3: third column) through an XZ view obtained at 488 nm (panel B) and 405 nm (panel C), respectively. The activation process is clearly not limited along the optical axis extending through the entire nucleus thickness. The low degree of colocalization in the merge of the 405 nm and 488 nm signals after the activation step evidenced a complete photoconversion of the paGFP molecules well beyond the focal plane (Fig. 1 panel D). When moving out of the cylinder defined by the ROIs some overlapping signals appeared: the tails of the point spread function (PSF) created by the excitation beam along the Z direction probably delivered an amount of energy not able to induce a complete conversion of the irradiated molecules in the border area of the illumination cone.

Optical confinement by evanescent field-induced photoactivation

TIRF microscopy can be successfully employed in photoactivation protocols exploiting its intrinsic spatial confinement along the *z*-axis. As a proof of principle for photoactivation-TIRF studies, U2OS osteosarcoma cells were transfected with EGFR-paGFP (epidermal growth factor receptor), fixed and imaged on a TIRF microscope (Fig. 2). Imaging of EGFR distribution on basal membrane by the evanescent field prior photoactivation at 488 nm reveals a very weak fluorescence signal due to the low absorbance peak of paGFP in its inactivated form both in TIRF (panel A) and widefield (panel B) observation conditions. In particular, the real EGFR distribution is, in this last case, almost completely masked by cell autofluorescence. After exposure to maximum energy flux of the violet excitation line under TIRF illumination, a progressive shift toward the 488-nm excitation peak is observed as demonstrated by a net 2- to 3-fold increase in the collected signal under TIRF conditions, proving that even an evanescent wave can induce photoactivation (Fig. 2 panel C) within controlled coupling and intensity conditions. One striking effect linked to photoactivation can be noticed by switching to a widefield fluorescence observation. Because activated molecules confined to the basal layer now produce an amplified amount of light, the net increase in contrast (Fig. 2 panel D) allows to gather a clear visualization of the real EGFR distribution on the basal layer visible out of the autofluorescence background. In this way, the two illumination schemes (TIRF and widefield) become equivalent, and widefield observation acquires a real increase in signal-to-noise ratio along the *z*-axis. Measurements on the photobleaching induced by the activating beam revealed a small effect on cells autofluorescence (about 2–3%). As a consequence, the increase in signal-to-noise ratio can be fully attributed to the photoconversion process of paGFP. The better confinement reached in TIRF-mediated activation

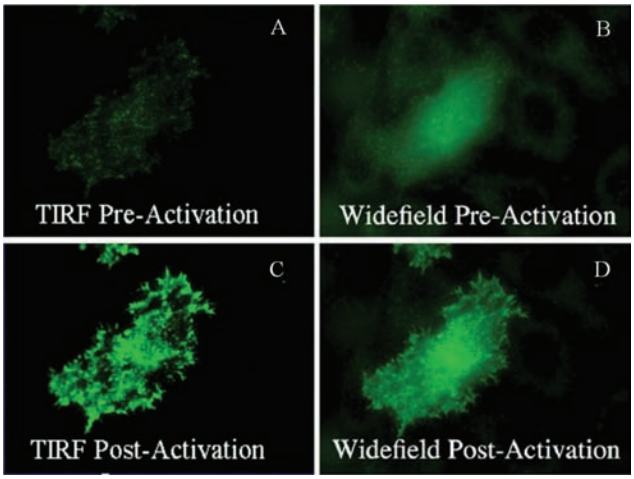

Fig. 2. Total internal reflection-based photoactivation. U2OS human osteosarcoma cells were transfected with EGFR-paGFP fusion protein to localize the paGFP moiety to plasma membrane. Fixed cells were then visualized by TIRF and widefield microscopy at 488 nm to monitor the effects of the exposure to a 405-nm evanescent field. Panel A and B show the low absorbance and the resulting poor signal-to-noise ratio of the paGFP molecules in native forms both under total internal reflection (A) and widefield (B) imaging conditions. Exposure to a violet evanescent field (15 s) produced a sharp increase in the emitted fluorescence measured as a 2.5-fold increase under TIRF 488 nm illumination (C). Post-activation widefield imaging at 488 nm (D) revealed a significative enhancement of signal-to-noise ratio making the basal membrane visible out of the autofluorescence background.

with respect to confocal microscopy set-up is demonstrated in Fig. 3. Cells were initially photoactivated by means of a 405-nm evanescent field and subsequently moved to a confocal microscope. After repositioning, a square region on the basal membrane has been re-exposed to 405-nm light using the violet laser of the confocal microscope (Fig. 3 panel A). Optical sectioning of the entire cell thickness revealed that activation with a Gaussian laser beam (Fig. 3 panel B and C, cyan arrow; Supplementary Movie available upon request as SM1) extended up to the apical membrane, whereas TIRF-activated field was efficiently confined to basal regions (magenta arrow) as evidenced in the graph in panel D where two intensity profiles running parallel to the optical axis has been plotted. The cyan profile measured through the area activated by means of the confocal laser beam (line positioned over the indicated cyan arrow along the XZ plane) clearly shows two peaks of comparable intensity in correspondence of the basal and apical membrane, respectively, whereas the TIRF activation profile (magenta line) presents only a single prominent maximum. A second peak in correspondence of the apical membrane is also present here: the signal is due to the not activated EGFR-paGFP molecules located on the upper face of the cell. Native paGFP is indeed able to emit green fluorescence when excited at 488 nm but with low efficiency. The relative height of the two peaks provides a ratio of about 3 times in agreement with the fold increase measurements of the evanescent-wave-induced activation mentioned above. The further increase in signal intensity of the photoactivated area on the confocal microscope with respect to the surrounding basal membrane surface photoactivated by the evanescent field suggests that TIRF illumination is not able to fully photoactivate the membrane molecules with the employed power.

To check the real activation depth and the possibility to discriminate basal layer even in complex expression patterns, cells were co-transfected for simultaneous expression of paGFP

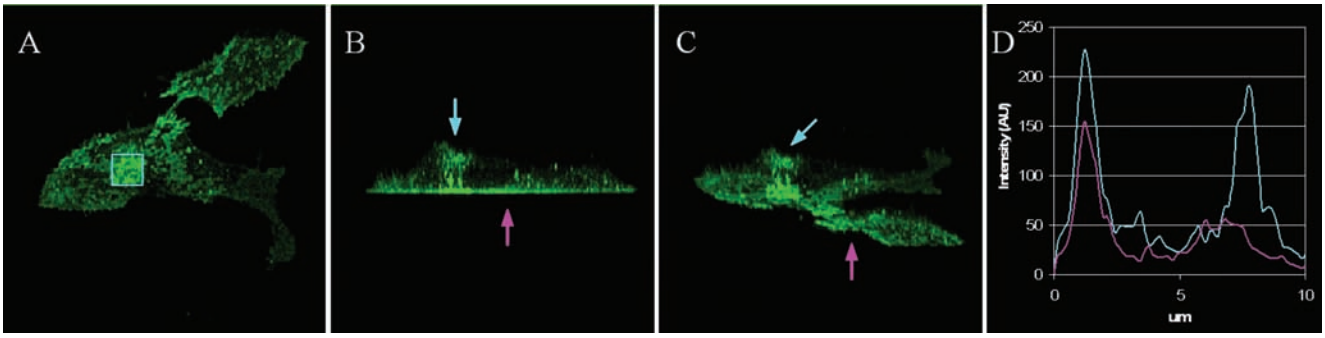

Fig. 3. Spatial confinement of photoactivation induced by an evanescent field analyzed by confocal microscopy. U2OS cells expressing EGFR-paGFP were photoactivated at 405 nm under total internal reflection conditions and subsequently moved to a confocal microscope for whole-cell optical sectioning analysis. A squared subregion on basal membrane (cyan square) has been activated using the confocal violet laser line to evaluate the different spatial confinement ability of the two techniques. The XY maximum intensity projection (MIP) of the collected stack (A) evidences the increased brightness of the area activated by the confocal Gaussian beam and the spatial confinement in the focal plane. XZ maximum intensity projection (B) through the activated area reveals that the area activated by the confocal laser beam (cyan arrow) extends from the basal to the apical membrane, whereas the rest of TIRF-photoconverted area (magenta arrow as a guide point) is limited to the lower membrane layer. A 30-degree rotated view along the Y direction (C) further evidenced how confocal microscopy activation extend up to apical membrane, whereas TIRF is efficiently confined on the basal layer. The graph in (D) reports the line intensity profiles along the arrows depicted in (B): the cyan curve measures the area activated in confocal microscopy, whereas the magenta curve is relative to the TIRF-photoconverted membrane portion.

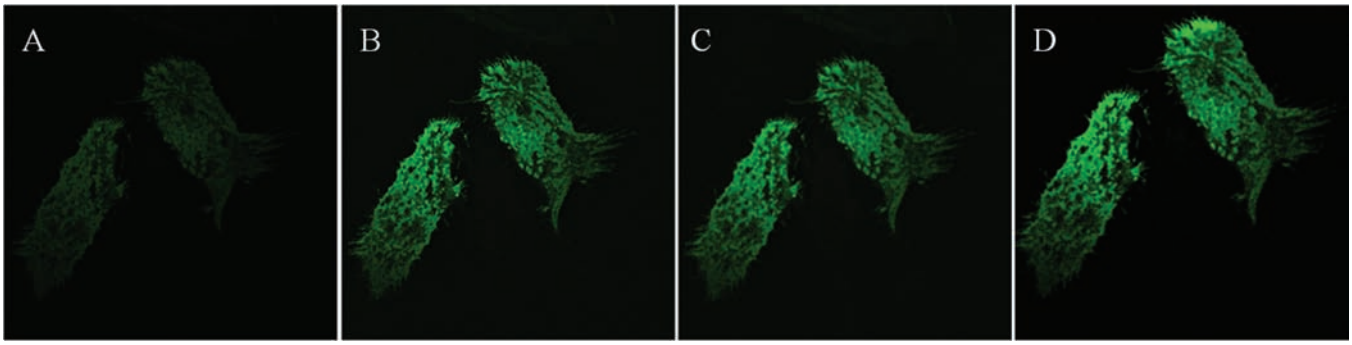

Fig. 4. Evanescent field-mediated photoactivation in complex expression patterns. U2OS cells were cotransfected to simultaneously express EGFR-paGFP and wild type paGFP. Because wild type paGFP protein is diffused everywhere within the cell, penetration of the photoconverting evanescent wave into the cell could be evidenced by an increased emission in fluorescence obscuring the basal layer in non-TIRF imaging conditions. The efficacy of the evanescent activating field (405 nm, 5-s exposure) is demonstrated by the sharp increase in intensity under 488 nm TIRF illumination before (A) and after (B) exposure to the violet light. Strikingly both widefield (C) and confocal (D) fluorescence imaging, which possesses a diminished axial resolution, exhibits the same spatial fluorescence distribution, suggesting that cytoplasmic paGFP located over the TIRF-activated layer was not involved in the photoconversion process.

and EGFR-paGFP fusion protein. Because wild type paGFP localizes throughout the entire cell volume, the activation thickness will be easily evidenced by the net increase in fluorescence throughout the internal cell body: if an extended portion above the TIRF plane was subjected to photoactivation, the resulting fluorescence should cause an obscuration of the EGFR distribution details when moving out the TIRF modality observation. Photoactivation under TIRF conditions (Fig. 4 panel A and B; 2.5–3 intensity fold increase) produced the same distribution pattern when observed in TIRF, widefield and confocal microscopy (Fig. 4 panel B, C and D, respectively) indicating that the paGFP molecules positioned above of the TIRF slice were not photoactivated by the exponential tail of the evanescent field. Analysis of activated cells on a confocal microscope (Fig. 5) strikingly demonstrated the efficiency of the photoactivation-TIRF protocol: activation in confocal microscopy can be efficiently confined to a limited area in the focal plane but it cannot avoid the spreading along the optical axis making the photomarking procedure unuseful (Fig. 5 panel A, B, C) for efficient targeting of the basal membrane. Molecules out of the focal plane in the targeted region of interest are activated producing a fluorescence signal able to mask the membrane distribution when a Gaussian laser beam is employed. The activated volume spreads throughout the entire cell thickness as demonstrated in the XZ view (cyan arrow) and by the corresponding intensity profile plotted in Fig. 5 panel D. The TIRF-activation profile (magenta curve) peaks in correspondence of the basal membrane and decay towards a plateau due to the fluorescence of the not activated paGFP molecules distributed throughout the cell. Again a 3-fold increase has been measured. Volume rendering (Fig. 5 panel C; Supplementary Movie available upon request as SM2) evidenced the efficacy of the confinement (Fig. 5 panel B and C, magenta arrow; panel D magenta intensity profile) under TIRF activation conditions. XZ view of a central slice cutting the area activated by the confocal beam clearly shows the photoconversion process through comparison of the 405-nm (Fig. 5 panel E) and 488-nm (Fig. 5 panel F) excitation after the activation step. Measurement of the extension of the photoconverted section along the XZ plane (Fig. 5 panel G) by a Gaussian fit of the membrane profile produced an average value of 570 nm very close to the axial resolution of a confocal microscope at 488 nm, suggesting that the real activation depth produced by the evanescent field could be confined to subresolution distances. TIRF microscopy possesses in fact an optical sectioning ability much higher than the confocal microscope due to the limited penetration depth producing a slice of 100–200 nm in comparison to the optical thickness of the section produced by a confocal microscope (about 1 micrometre).

In the cotransfection of two different constructs, control of the relative amount of proteins could represent a quite difficult task. Consequently, the preferential membrane localization of EGFR-paGFP could in some way create a bias in the observed results. The enhancement of contrast making the widefield and TIRF imaging similar has been indeed observed in U2OS cells expressing wild type paGFP only, excluding potential artefacts related to spatial concentration of the employed constructs. Activation the paGFP molecules in the TIRF layer produced a signal able to overcome the diffuse light coming from the native population therefore leading to a virtual sectioning effect of the basal layer of the cell (Supplementary Movie SM3). To further check that TIRF-confined photoactivation can translate this increased ability to confocal microscopy, a more physiological model was analyzed. HeLa cells expressing p52SHC-paGFP fusion protein (Fig. 6) were activated by the evanescent field under total internal reflection conditions (Fig. 6B) and then moved to a confocal microscope. p52SHC is a protein involved in signal transduction interacting with phosphorylated tyrosine residues of plasma membrane

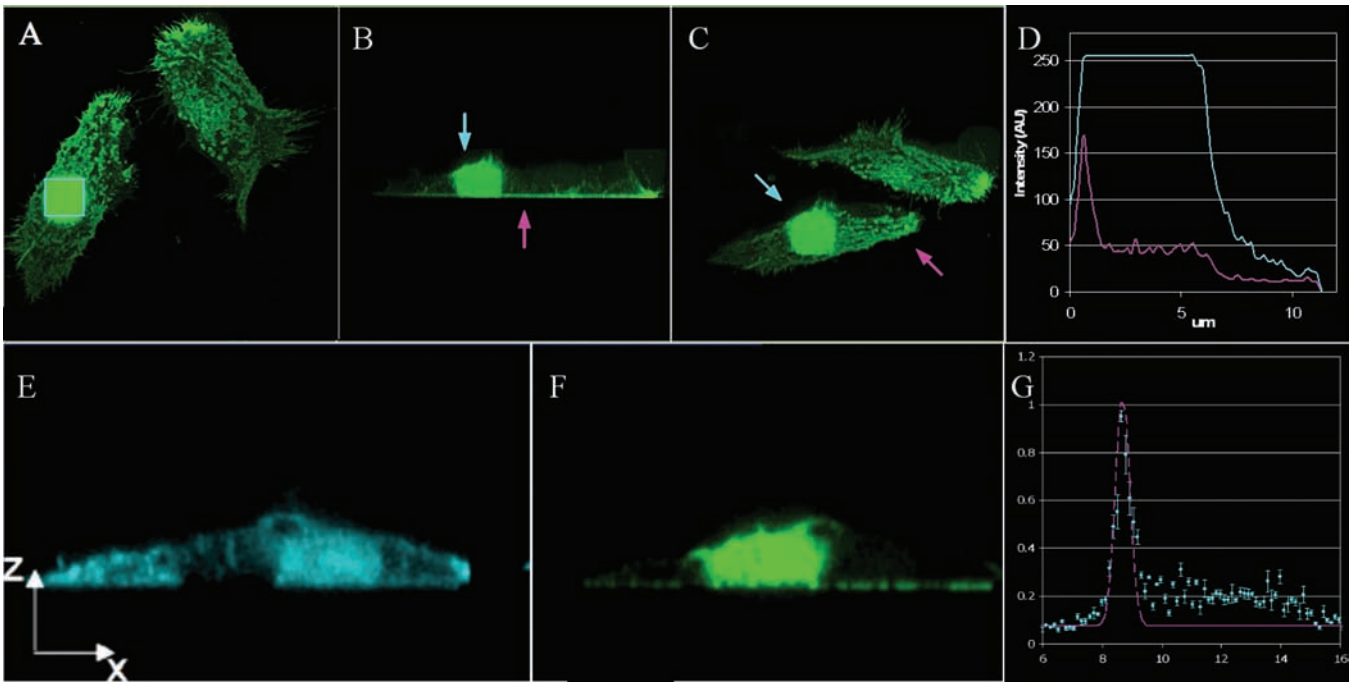

Fig. 5. Confocal microscopy analysis of TIRF-photoactivation confinement in complex expression patterns. U2OS cells were cotransfected to simultaneously express EGFR-paGFP and wild type paGFP, activated under TIRF conditions and then moved to a confocal microscope where the confined region of interest showed in the XY MIP (A) was reactivated (cyan square). When the extent of the photoactivation along the optical axis was examined by confocal microscopy through a XZ MIP (B), the efficient confinement of TIRF photoactivation (magenta arrow) with respect to Gaussian beams (cyan arrow) was evident, as confirmed in volume rotation view reported in (C). The graph in (D) reports the line intensity profiles along the arrows depicted in (B): the cyan curve measures the area activated in confocal microscopy, whereas the magenta curve is relative to the TIRF-photoconverted portion. The slow and almost flat decay of the curve running through the TIRF-activated area is due to the fluorescence of the high number of not-activated paGFP molecules in the cell cytoplasm. XZ planes along the activated region at low 405-nm (E) and 488-nm excitation (F) evidenced the photoconversion extent. The graph in (G) reports the intensity profile along the membrane and a Gaussian fit (dashed line) providing a FWHM of 570 nm. The measured value is very close to the axial resolution limit of a confocal microscope suggesting that the evanescent field activation extent could be limited to subdiffraction values.

receptor tyrosine kinases: upon overexpression, its signal is spread throughout the cell cytoplasm (Fig. 6 panel A inset) with only a minor fraction recruited to the plasma membrane making TIRF microscopy the only tool able to discriminate the molecules recruited to the receptors. Illumination of basal layer with moderate 405-nm excitation energy (Fig. 6C) shows the optical slice thickness typical of the confocal microscope and of its reduced axial resolution in comparison to TIRF microscopy (Fig. 6B): the high number of molecules present in the confocal layer produce a high background masking the protein distribution in proximity of the basal membrane. Following photoactivation, the higher signal-to-noise ratio in the TIRF plane produces an increased sectioning ability (Fig. 6D) when molecules are observed at 488 nm, making the two optical schemes equivalent under the adopted conditions. The number of photons emitted by the p52SHC-paGFP molecules located in the TIRF slice is now able to overcome the signal produced by the native paGFP present in the confocal volume producing a change in measured distribution well evident from comparison of panel C and D. The absolute measurement of the real penetration and activation depth cannot be inferred from the presented data. Such data demonstrate that the photoconversion process can be efficiently confined making the confocal and TIRF observation scheme equivalent creating a single (photoactivated) optical section of reduced thickness.

The measurement of the photophysical behaviour of paGFP protein in terms of activated slice depth and photostability under TIRF conditions forced us to work on fixed samples to avoid the influence of molecular mobility on the result of the photoconversion process. To validate the obtained observations and applicability of paGFP photoactivation by evanescent waves *in vivo*, U2OS cells living cells were exposed to high-energy 405-nm fluxes at 1 s intervals for 20 s. The measured fold increase is compatible with the one measured on fixed samples, whereas no phototoxicity effects were observed on the cells exposed to the violet activating light. In order to provide an example of potential applications for biomedicine in living cells, a field diaphragm has been introduced in the optical 405-nm TIRF pathway in order to limit the photoconversion

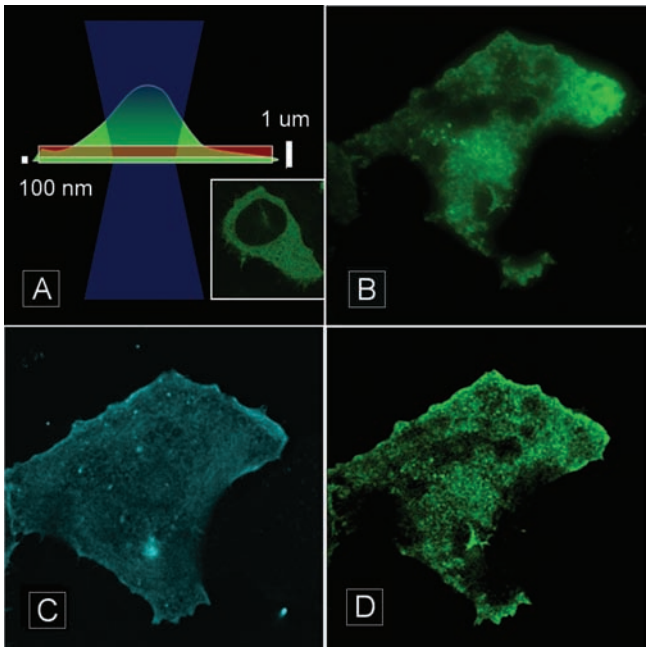

Fig. 6. TIRF-confined photoactivation gives confocal microscopy-increased sectioning ability. Confocal microscopy optical sectioning is based on spatial filtering by emission pinhole giving an optical slice thickness of approximately 1 um (A), with an opening of 1 Airy unit. The complex expression pattern produced by p52SHC-paGFP fusion protein upon overexpression (A, inset) does not consequently allow to discriminate between the membrane located fraction due to the fluorescence of the high number of molecules present in the cytoplasm without the help of TIRF microscopy (B). Basal layer imaging at 405 nm before photoconversion was consequently the result of superposition of light coming from such an extended intracellular portion (C) and is not able to produce a comparable distribution to TIRF imaging. However, when an evanescent field was applied for photoactivation, paGFP molecules on a much limited portion (100–200 nm) produced a much higher extent of photons obscuring the remaining signal contained in the confocally sectioned images (1 μm), making TIRF (B) and confocal microsopy (D) essentially equivalent.

process in the XY plane. Once reached the maximal activation value (about 3-fold increase), cells were only imaged with 488-nm line to follow diffusion of the activated EGFR-paGFP molecules. Fig. 7 presents the time-dependent redistribution of the fluorescence signal: the intensity profile of the activated region first increases during the exposure to violet radiation and suddenly decreases when the activating light has been switched off. A corresponding increase in fluorescence out of the photoactivated region enclosed by the diaphragm demonstrates that the signal decay is due to the molecules redistribution upon diffusion across the cell membrane and not to photobleaching effects.

Optical confinement by two-photon-induced photoactivation

The relevant limitation of TIRF is the inability to move apart from the basal membrane to penetrate into the cell as in confocal microscopy-based optical sectioning. Moreover, the increase in contrast gained at the basal membrane can be easily lost when switching to widefield fluorescence analysis once molecules were internalized due to the poor optical sectioning ability of this technique. TIRF also pays to scanning techniques the price of a lack of easy and efficient confinement in the plane to selectively mark arbitrary-shaped structures.

Non-linear excitation techniques, such as 2PE laser scanning microscopy, allow to overcome this limit achieving a real 3D reconstruction ability based on a true spatial confinement along the three dimensions (Diaspro *et al.*, 2005). Two-photon absorption is, according to the rules of quantum mechanics, a low probability event requiring an incredibly high amount of photons. Consequently, only those fluorescent molecules located in the optical focal plane of the microscope objective are excited by the simultaneous absorption of two low-energy photons. Rapid decay of activation efficiency as function of the distance from the objective focus provides a spatial confinement that can be employed both for fluorescence excitation and photoactivation. In a previous paper (Schneider *et al.*, 2005), we clearly demonstrated that two-photon activation of paGFP is indeed possible at appreciable efficiency between 720 nm and 840 nm, whereas the activated molecules exhibited photophysical properties very similar to eGFP with an absorption peak at >900 nm. It is consequently possible to perform photomarking with infrared lasers, employing the confinement effect of non-linear excitation and its reduced phototoxicity with respect to violet light, whereas switching to one-photon observation for tracking activated molecules at 488 nm.

Figure 8 (panel 1) shows two-photon photoactivation of EGFR-paGFP protein in different cell regions. The photoactivation process can be extended to any region within the specimen with an intrinsic 3D confinement allowing for selective excitation of either the basal (Fig. 8 panel 1–A XY view; panel 1–B XZ view), middle height (Fig. 8 panel 1–C XY view; panel 1–D XZ view) and apical membrane (Fig. 8 panel 1–E XY view; panel 1–F XZ view).

Optical sectioning ability of two-photon microscopy can provide a more complete description of biophysical phenomena when compared to TIRF even in presence of a diminished optical resolution and spatial confinement as in the case of molecular diffusion studies in cell membranes. TIRF-photoactivation analysis revealed a continuous diffusion of the receptor through the basal membrane (Fig. 7). Studies of EGFR mobility properties can be extended by two-photon-induced activation to different cell membrane regions. In fact, 3D confined regions can be consequently activated on the basal membrane (Fig. 8 panel 2 ROI1) and along the plasma membrane at different positions along the optical axis (Fig. 8 panel 2, ROI2–4). The speed of intensity redistribution can be monitored (graph in Fig. 8 panel 2; Supplementary Movie available upon request as SM4) and diffusion of signal over time measured to obtain a rough estimation of the molecular

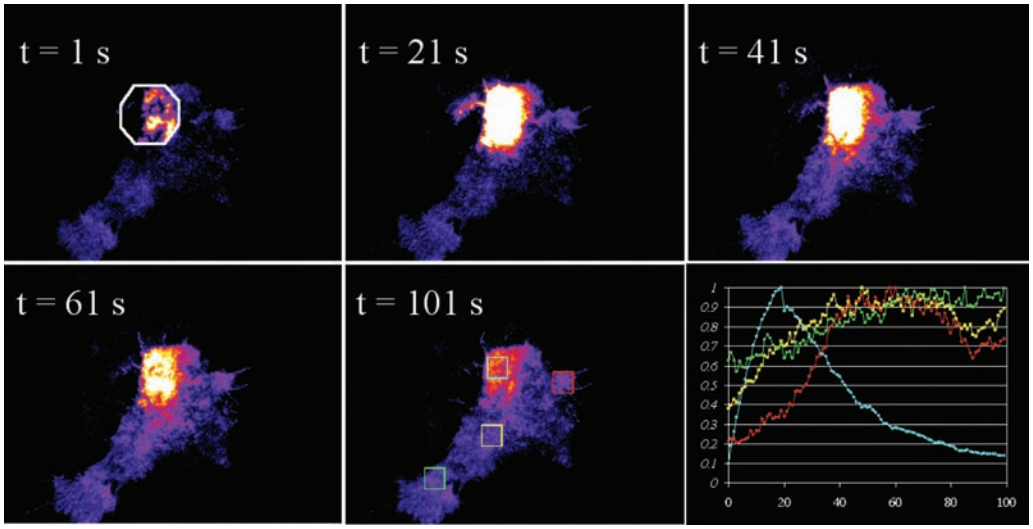

Fig. 7. EGFR-paGFP photoactivation in living cells. U2OS cells were transfected with EGFR-paGFP encoding DNA and imaged in TIRF microscopy to monitor the efficiency of evanescent wave-mediated photoactivation in living cells and to measure the influence of molecular mobility on the results of the activation process. A field diaphragm (drawn in the 1-s image) has been inserted in the 405-nm TIRF optical pathway to limit the photoactivated area extension in the focal plane. After 20 repeated cycles of stimulation through a 1-s exposure to 405-nm illumination for activation and subsequent imaging at 488 nm, the cells were only imaged at 1-s time intervals. The reported images at the indicated time points provide representative examples of the temporal kinetics reported in the graph. Monitoring of the intensity through the ROIs depicted in the image collected at the end of the process (101 s) revealed the redistribution of the activated molecules through the plasma membrane due to the receptor diffusion.

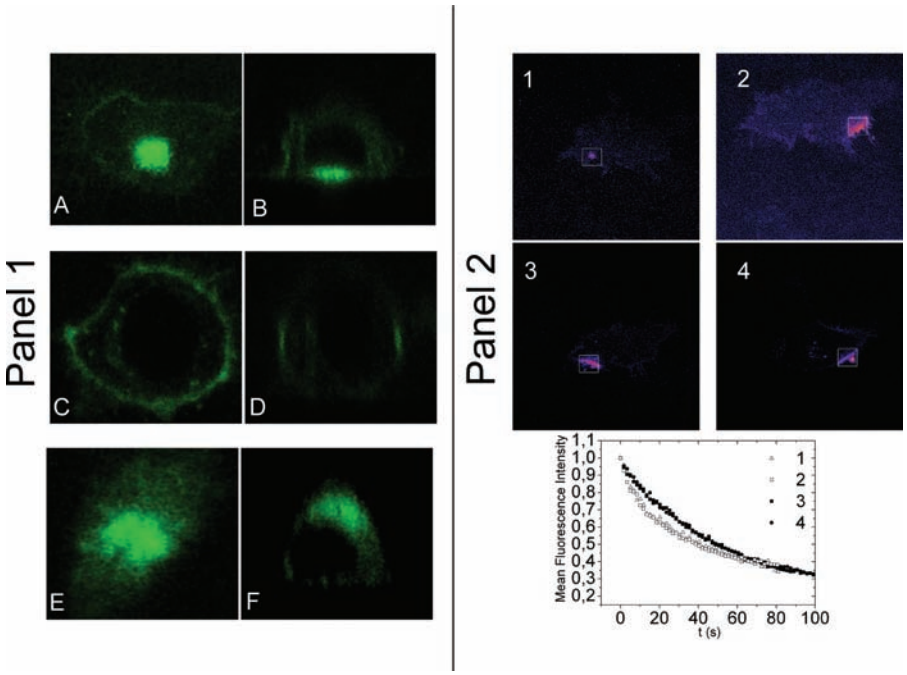

Fig. 8. Two-photon activation allows real control of the photoconverted volume in three dimensions. Panel 1. Spatial confinement of two-photon-induced photoactivation in HeLa cells expressing EGFR-paGFP. Basal (A), middle (C) and apical (E) membrane portions were photoactivated at 750 nm with a pulsed infrared laser and imaged by 488-nm light. XZ views (B, D, F) show the spatial confinement of the activated areas along the optical axis. Panel 2. Characterization of diffusion properties in different cell regions employing two-photon-modulated photoactivation. HeLa cells transiently transfected with EGFR-paGFP were analyzed to estimate mobility of the receptor under exponential growing conditions. Different areas at different heights (starting from basal towards apical membrane: ROI1–4) on cell membrane were photoactivated with two-photon microscopy to analyze the signal temporal evolution. Plotting of the decay curves revealed similar kinetics temporal evolution with a single-exponential behaviour.

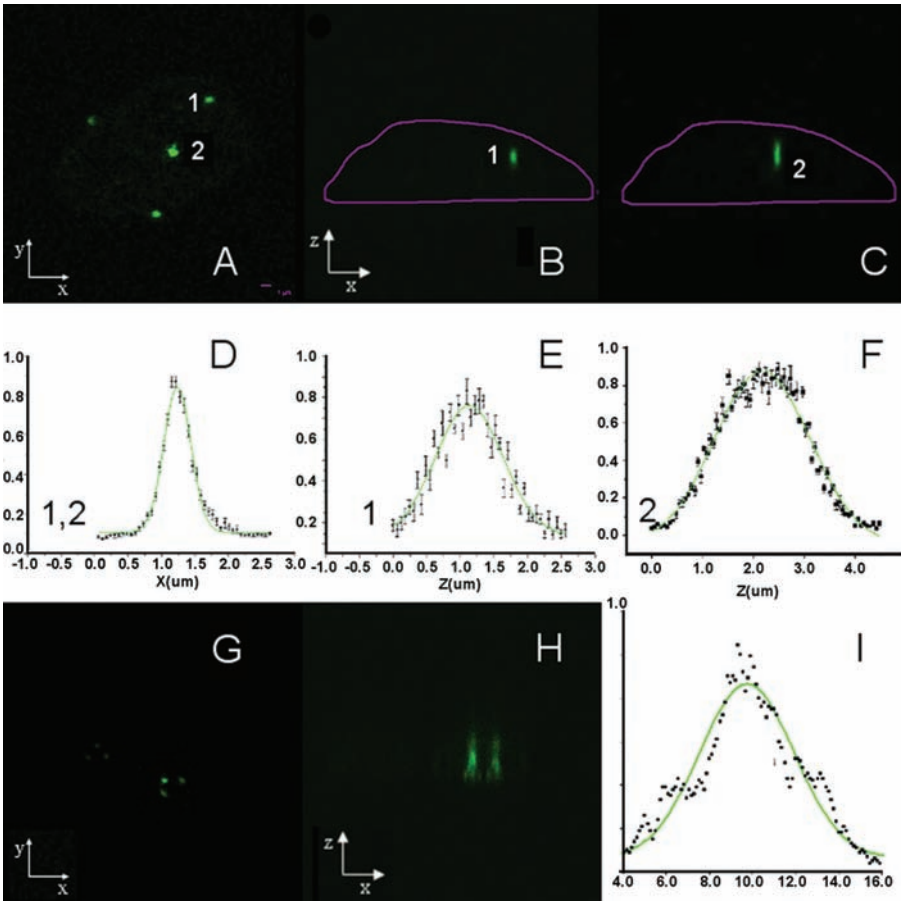

Fig. 9. Controlling the activation volume by two-photon-induced photoactivation. HeLa cells expressing H2B-paGFP were photoactivated employing a 750-nm wavelength and imaged by 488-nm light. Photoactivation has been obtained parking the beam on a single point in the field of view for different activation times (ROI1: 1 s; ROI2: 3 s) to study spatial confinement in dependence of the amount of delivered energy. A full width half maximum (FWHM) of the activation profile (A) around 400 nm (D: Gaussian fit results) has been measured in the XY plane independently from the employed activation energy. This value is in perfect agreement with the theoretical resolution limit provided by two-photon microscopy indicating that the activated volume is a representation of the system point spread function. The extension of the axial activation profile shows, however, a variation according to the two-photon energy flux passing from 1 (B, E: Gaussian fit) to 2 um (C, F: Gaussian fit) FWHM value. Repetition of the same experiment focusing a single point in the xy plane (G) with one-photon confocal microscopy provided an axial extension (H) that can be hardly fitted by a Gaussian profile due to its extension spanning throughout the entire nucleus. An indicative value for FWHM can be estimated around 6 um (I: Gaussian fit).

mobility of the receptor in the different membrane spatial compartments.

Self-assembled structures characterized by a low exchange rate of their components with the external environment can be efficiently marked creating fusion proteins with the paGFP moiety. Multiphoton excitation provides not only the peculiar advantage of a confined photoactivation but also the possibility to vary the extent of the 3D activation by modulating the illumination power and time. In order to study such a process and measure the minimal activatable spatial extent in living cell-based applications, HeLa cells were transfected with an H2B-paGFP chimeric construct. In this case, the molecular diffusion of the marked histone is slow and allows for the specific labelling of targeted nuclear areas, because no consistent signal reduction over activated areas can be recorded over several minutes. Different activation energies were applied by time-power control and the resulting radial and axial intensity profiles evaluated. Heterochromatin-rich regions (the brighter spots of highly condensed DNA visible, e.g. in Fig. 1) of suitable size were targeted in order to avoid potential artefacts due to spatial concentration gradients [the very same observations were confirmed in fixed paGFP expressing HeLa cells employing the quite homogenous distribution of the protein to further exclude a bias related to the spatial distribution of the H2B-paGFP construct (Supplementary Movies SM5, SM6; Supplementary Figures 1, 2, 3)]. Figure 9 reports the result of the activation of a single pointed spot in the scanned region obtained by parking the infrared laser beam with different exposure time in order to monitor the photoactivation dependency with respect to the released

energy (Fig. 9; region 1: 1 s; region 2: 2 s; panel A: XY view; panel B and C: XZ view). The same cell was then excited at $\lambda =$ 488 nm and a stack running through its entire depth acquired. The intensity profiles reported in panel D and E provided a full half width maximum (FHWM) of about 400 nm in the x direction for both the activated areas independently from the applied energy and 1000 nm along the axial direction for the region 1. Photoactivation of a single pointed spot through the above-mentioned procedure results in an image of the so-called 3D PSF providing a measurement of the spatial resolution of the system. The comparison to single-photon PSF evidenced a lower resolution due to the almost doubled exciation wavelength, a well-known price paid by multiphoton microscopy to the conventional techniques. However, the small reduction in lateral resolution disappears looking at the XZ profiles measured: variations in the employed activating energy allow to modulate the axial extent from 1 to 2 μm with an accurate control of the spatial confinement (Fig. 9, panel E and F). Repetition of the experiment employing single-photon excitation (Fig. 9, panel G: xy view; panel H: xz view) revealed an xz profile spanning throughout the whole nucleus thickness, with a putative FHWM greater than 6 μm (Fig. 9, panel I).

Discussion

Photoactivatable green fluorescent protein and other photoactivatable/convertible proteins provide a comparatively new efficient tool for characterization of molecular events in living cells and organisms. However, limitations mainly stem from the inefficacy of widefield and confocal microscopy to control the 3D extent of activated GFPs within the specimen. New optical tools are consequently desirable for more precise targeting of the cellular compartments containing the proteins of interest.

We demonstrated here that both TIRF and two-photon excitation microscopy can be successfully employed to confine photoactivation within the three spatial dimensions. A 405-nm evanescent field created under total internal reflection regime is able to photoactivate paGFPs within a depth of few hundreds nanometres in comparison to the much wider range obtained in confocal microscopy. The presented data demonstrate the possibility and usefulness to employ TIRF in photoactivation processes for studying dynamics events in proximity of the basal membrane with molecular resolution. Unfortunately, the TIRF approach suffers of the intrinsic confinement to cell-substrate adhesion areas and a low flexibility in modulation in the focal plane. In fact, the use of a field diaphragm can limit the planar extension of the illuminated area but it cannot ensure the flexibility typical of scanning techniques in which the point-by-point illumination control allows to dose energy over arbitrary shaped regions within a 3D specimen. Two-photon excitation microscopy, utilized in the activation mode, allows removal of such limitations enabling to couple optical sectioning ability with a fine three-dimensional control of photoactivatable volumes.

A remarkable effect linked to the usage of axially confined activation can be discerned from the measured data. When TIRF is used to activate paGFP molecules on the cell basal membrane, only those molecules become actually visible when switching to widefield or confocal observation. Consequently, the effect is equivalent to image a fluorescent layer of approximately 100–200 nm, because the outer molecules, unconverted, cannot be efficiently excited by a 488-nm light source. The theoretical optical thickness of a slice taken by a confocal microscope in correspondence of excitation and emission parameters of GFP is in the micrometre range demonstrating the increased sectioning ability achieved by the TIRF-confocal combination. A similar situation can be fulfilled in a correlative light and electron microscopy approach. In this case, fine physical slicing of samples with a subresolved thickness (about 200 nm) in preparation to electron microscopy examination grants a better optical microscopy analysis (Robinson *et al.*, 2001). In the case of axially confined photoactivation, the cutting effect is reached by limiting the photoconversion process to a very thin layer creating a subresolved optical slice instead of a physical one, envisaging the use of the photoactivation process as a tool to enhance the performances of the optical system. A parallel can be made with PALM (Betzig *et al.*, 2006), another recent application where photoactivation is employed to visualize molecules at nanoscale resolution. Photo activation localization microscopy (PALM) is based on the use of TIRF for imaging detection on cut slice of subresolution thickness where photoactivation is obtained by a focused Gaussian laser beam, making our approach extremely different. Even if TIRF confined photoactivation cannot grant the resolution typical of PALM, it can employ its peculiarity of living cell compatibility for dynamic tracking thanks to the localized increase in signal-to-noise ratio maintained when moving out of the TIRF imaging conditions.

The presented data evidenced a limitation stemming from the employed fluorescent molecules: native and activated paGFP molecules possess the same emission spectra. Consequently, the highlighting effect linked to photoactivation is only based on a different number of photons related to the variation in absorption spectra. Not activated molecules will consequently contribute to establish the background threshold and the relative number and distribution of activated versus not-activated proteins will affect the best signal-to-noise ratio and its time decay. One possible solution can be represented by PS-CFP2 photoswitchable fluorescent protein, which presents very similar photophysical properties with respect to paGFP but with a fundamental switch in the emitted light colour between native and activated form. The measured fold-increase in the evanescent field-induced photoactivation (2–3 times) could be consequently enhanced by reducing the background level exploiting the different emission of the two forms.

Two-photon excitation microscopy, despite its lower optical resolution, clearly demonstrates its superior ability to control the photoactivation volume providing additional clues into functional analysis of molecular events. Modelling of diffusion properties of molecules based on photoactivation/photobleaching protocols in conventional widefield or confocal fluorescence microscopy is generally limited to a 2D geometry assumption that is not completely verified due to the extent of the activation/bleaching process along the optical axis. This limitation can be fully removed under non-linear regime, i.e. two-photon photoactivation. It is worth noting that the 3D confinement attainable under two-photon regime opens an important window on the characterization of the properties of cellular compartments in a way not achievable by conventional techniques. We demonstrated how different areas on basal and apical membrane can be efficiently activated allowing for a local analysis of the diffusion coefficient. In fact, such an application is immediately endowed of a great value when applied, e.g. to specific biological models where polarization of membranes creates a real meaningful distinction between the two differently located membrane compartments. In this context, new 3D analysis models can be consequently tested coupling confined fluorescence photoactivation to fast scanning techniques.

In conclusion, the development of protocols for spatially localized photoactivation of fluorescent molecules is of great impact also considering the growing number of photoactivatable proteins. The ability of performing 3D photochemistry assumes a not-commensurable value. Besides spatial confinement, operating under two-photon regime is convenient for simultaneous activation of different molecules exploiting the overlapping properties of the two-photon cross-sections (16).

Acknowledgements

This work was supported by IFOM (FIRC Institute of Molecular Oncology, Milan, Italy), by Fondazione Compagnia di San Paolo (Turin, Italy) and by AD PRIN2006-MiUR (2006028909 Ministry of University and Research). The authors are indebted to George Patterson and Jennifer Lippincott-Schwartz for paGFP availability.

References

Axelrod, D. (2003) Total internal reflection fluorescence microscopy in cell biology. *Methods Enzymol.* **361**, 1–33.

Beaudouin, J., Mora-Bermudez, F., Klee, T., Daigle, N. & Ellenberg, J. (2006) Dissecting the contribution of diffusion and interactions to the mobility of nuclear proteins. *Biophys. J.* **90**, 1878–1894.

Betzig, E., Patterson, G.H., Sougrat, R. *et al.* (2006) Imaging intracellular fluorescent proteins at nanometer resolution. *Science* **313**, 1642–1645.

Chudakov, D.M., Verkhusha, V.V., Staroverov, D.B., Souslova, E.A., Lukyanov, S. & Lukyanov, K.A. (2004) Photoswitchable cyan fluorescent protein for protein tracking. *Nat. Biotechnol.* **22**, 1435–1439.

Conchello, J.A. & Lichtman, J.W. (2005) Optical sectioning microscopy. *Nat. Methods* **2**, 920–931.

Diaspro, A., Chirico, G. & Collini, M. (2005) Two-photon fluorescence excitation and related techniques in biological microscopy. *Q. Rev. Biophys.* **38**, 97–166.

Lippincott-Schwartz, J., Altan-Bonnet, N. & Patterson, G.H. (2003) Photobleaching and photoactivation: following protein dynamics in living cells. *Nat. Cell. Biol.* **Suppl**, S7–14.

Misteli, T. (2001) The concept of self-organization in cellular architecture. *J. Cell. Biol.* **155**, 181–185.

Mutoh, T., Miyata, T., Kashiwagi, S., Miyawaki, A. & Ogawa, M. (2006) Dynamic behavior of individual cells in developing organotypic brain slices revealed by the photoconvertable protein Kaede. *Exp. Neurol.* **200**(2), 430–437.

Patterson, G.H. & Lippincott-Schwartz, J. (2002) A photoactivatable GFP for selective photolabeling of proteins and cells. *Science* **297**, 1873–1877.

Patterson, G.H. & Lippincott-Schwartz, J. (2004) Selective photolabeling of proteins using photoactivatable GFP. *Methods* **32**, 445–450.

Robinson, J.M., Takizawa, T., Pombo, A. & Cook, P.R. (2001) Correlative fluorescence and electron microscopy on ultrathin cryosections: bridging the resolution gap. *J. Histochem. Cytochem.* **49**, 803–808.

Sako, Y., Ichinose, J., Morimatsu, M., Ohta, K. & Uyemura, T. (2003) Optical bioimaging: from living tissue to a single molecule: single-molecule visualization of cell signaling processes of epidermal growth factor receptor. *J. Pharmacol. Sci.* **93**, 253–258.

Sato, T., Takahoko, M. & Okamoto, H. (2006) HuC:Kaede, a useful tool to label neural morphologies in networks in vivo. *Genesis* **44**, 136–142.

Schneider, M., Barozzi, S., Testa, I., Faretta, M. & Diaspro, A. (2005) Two-photon activation and excitation properties of PA-GFP in the 720-920-nm region. *Biophys. J.* **89**, 1346–1352.

Thoumine, O., Lambert, M., Mege, R.M. & Choquet, D. (2006) Regulation of N-cadherin dynamics at neuronal contacts by ligand binding and cytoskeletal coupling. *Mol. Biol. Cell.* **17**, 862–875.

Willig, K.I., Kellner, R.R., Medda, R., Hein, B., Jakobs, S. & Hell, S.W. (2006) Nanoscale resolution in GFP-based microscopy. *Nat. Methods* **3**, 721–723.

Yuste, R. (2005) Fluorescence microscopy today. *Nat. Methods* **2**, 902–904.

Supplementary Material

The following supplementary material is available for this article:

Supplementary Figure 1. Spatial confinement of 2p-induced photoactivation (I): Preactivation images of Hela cell expressing paGFPs molecules. Each image represents an xy plane ($61.5 \times 61.5\,\mu$m, 512×512 pixels) collected at different z level from basal to apical plasma membrane. We insert, as Supplementary Movies 5, the whole 3D stack performed collecting the images each 200 nm along the optical axis.

Supplementary Figure 2. Spatial confinement of 2p-induced photoactivation (II): the same cell of Supplementary Figure 1 after a pulse of activation obtained parking the beam on a single point (40 ms, P∼40mW, $\lambda = 800$ nm, yellow circle). We insert, as Supplementary Movies 6, the whole 3D stack performed collecting the images each 200 nm along the optical axis after inducing activation.

Supplementary Figure 3. Spatial confinement of 2p-induced photoactivation (III): A full width half maximum (FWHM) of the activation profile (graph a) around 360 nm (Gaussian fit results) has been measured in the x direction. This value is in agreement with the theoretical resolution limit provided by two-photon microscopy indicating that the activated volume is a representation of the system PSF. The axial activation profile shows an extension of 0.8–1 μm (Gaussian fit results, graph b). The image c (30.76 μm) represents an xz view of the previous cell after inducing activation.

Supplementary movies available upon request

Supplementary Movie 1. TIRF-confined photoactivation. Volume rendering of TIRF-activated EGFR-paGFP.

Supplementary Movie 2. TIRF-confined photoactivation. Volume rendering of TIRF-activated EGFR-paGFP in U2OS cells expressing paGFP wt and EGFR-paGFP.

Supplementary Movie 3. TIRF-confined photoactivation in paGFP-expressing cells. U2OS cells expressing paGFP alone were exposed for 1 s to 405 nm light and then excited with blue light to collect TIRF (up) and widefield (down) images. The procedure has been repeated for 20 cycles.

Supplementary Movie 4. EGFR-paGFP diffusion measured by two-photon confined photoactivation.

Supplementary Movie 5. 3D stack of Hela cell expressing paGFP alone. We collected images of 61.5×61.5 μm, sampling each 200 nm along the optical axis.

Supplementary Movie 6. 3D stack performed on the same cell and with the same parameters of Supplementary Movie 5 after a confined activation pulse.

This material is available as part of the online article from: http://www.blackwell-synergy.com/doi/abs/10.1111/j3635-2818.2008.1951.x
(This link will take you to article abstract).

Please note: Blackwell Publishing are not responsible for the content or functionality of any supplementary materials supplied by authors. Any queries (other than missing material) should be directed to the corresponding author for the article.

